Journal of Trace Elements in Medicine and Biology 52 (2019) 126–135

Contents lists available at ScienceDirect

Journal of Trace Elements in Medicine and Biology

journal homepage: www.elsevier.com/locate/jtemb

Toxicology

# Cerium ion promotes the osteoclastogenesis through the induction of reactive oxygen species

Lan Zhou[a,1], Shupei Tang[b,1], Lu Yang[a], Xiaoyong Huang[b], Ling Zou[a], Yu Huang[c], Shiwu Dong[a], Xinyuan Zhou[b,*], Xiaochao Yang[a,*]

[a] School of Biomedical Engineering and Medical Imaging, Third Military Medical University, China
[b] Institute of Immunology, Third Military Medical University, China
[c] Department of Gastroenterology, Xinqiao Hospital, Third Military Medical University, China

ARTICLE INFO

*Keywords:*
Cerium
Osteoclast
Osteoclastogenesis
Reactive oxygen species

ABSTRACT

Cerium and cerium containing materials have been drawing increasing attentions in industrial and biomedical applications in recent decades. The increased applications of cerium have also increased the risk of human body exposed to cerium ions. Due to its similar ionic radius to calcium(II), cerium(III) have found mainly deposited in the skeletal system. However, the effects of cerium(III) on the bone metabolism homeostasis remain poorly understood. In the present study, the effect of cerium(III) on the osteoclastogenesis which plays a pivotal role in bone metabolism homeostasis was investigated. Cerium(III) could enhance the expression and activity of NADPH oxidase1 (Nox1) leading to the elevation of intracellular reactive oxygen species (ROS) level. The augmentation of ROS level activated the RANKL dependent osteoclasts differentiation pathways resulted in the promotion of osteoclastogenesis, while anions associated with cerium(III) cation have no effects on the differentiation of osteoclasts. The cerium(III) activated osteoclasts exhibited enhanced bone resorption capability. These results provided fundamental information for understanding the potential effects of cerium(III) on the metabolism homeostasis of skeletal system which is of great reference value for future biomedical applications of cerium salts.

## 1. Introduction

Cerium is the most abundant rare earth element which makes up about 0.0046% wt of the Earth's crust [1]. The abundant reserves of cerium and the unique chemical properties of cerium containing materials have driven the intensive studies on exploring the application of these materials. Accordingly, cerium containing materials have been engineered for application in areas as diverse as automobile exhaust treatment, fuel cells, water-gas shift, and photocatalytic degradation [2–5].

In their natural occurrence, cerium has trivalent and tetravalent states. However, cerium ion in tetravalent state is unstable in the solution with pH > 3.0 [6]. The ionic radius of cerium(III) (1.01 Å) is very close to that of the calcium(II) (1.00 Å). This similarity enables cerium (III) the capability to replace calcium(II) in many calcium-containing biomolecules leading to the change of bioactivities of these biomolecules [6]. This unique biochemical property of cerium(III) has been developed for applications in antiemetic, prevention of postburn sepsis and inflammatory [7–9]. Several cerium salts including chloride, nitrate and stearate were known for their antibacterial activity.

Nevertheless, some studies have also reported the toxicity concerns of cerium(III). For example, recent studies have revealed that cerium (III) could induce pulmonary inflammation, liver injury, hippocampus injury, muscle paralysis and kidney injury in animal models [10–14]. These studies implied that the effects of cerium(III) on different organs have to be comprehensively evaluated before the cerium containing materials can be safely applied to the human body.

Skeletal system which makes up the framework of human body is one of the most important organs. Skeletal system health is highly dependent on the bone metabolism homeostasis regulated by the osteoclastic bone resorption and osteoblastic bone formation processes [15]. Bone metabolism disorder can cause many diseases such as osteoporosis, rheumatoid arthritis and osteopetrosis [16–18]. Thus, maintaining the normal activity of osteoclasts and osteoblasts is of great importance to skeletal system health. Cerium ions have found mainly deposited in the skeletal system [6]. If excessive cerium(III) is existed,

* Corresponding authors.
*E-mail addresses:* xinyuanzhou@tmmu.edu.cn (X. Zhou), xcyang@tmmu.edu.cn (X. Yang).
[1] These authors ranks equally in the first position of this publication.

https://doi.org/10.1016/j.jtemb.2018.12.006
Received 25 September 2018; Received in revised form 23 November 2018; Accepted 10 December 2018

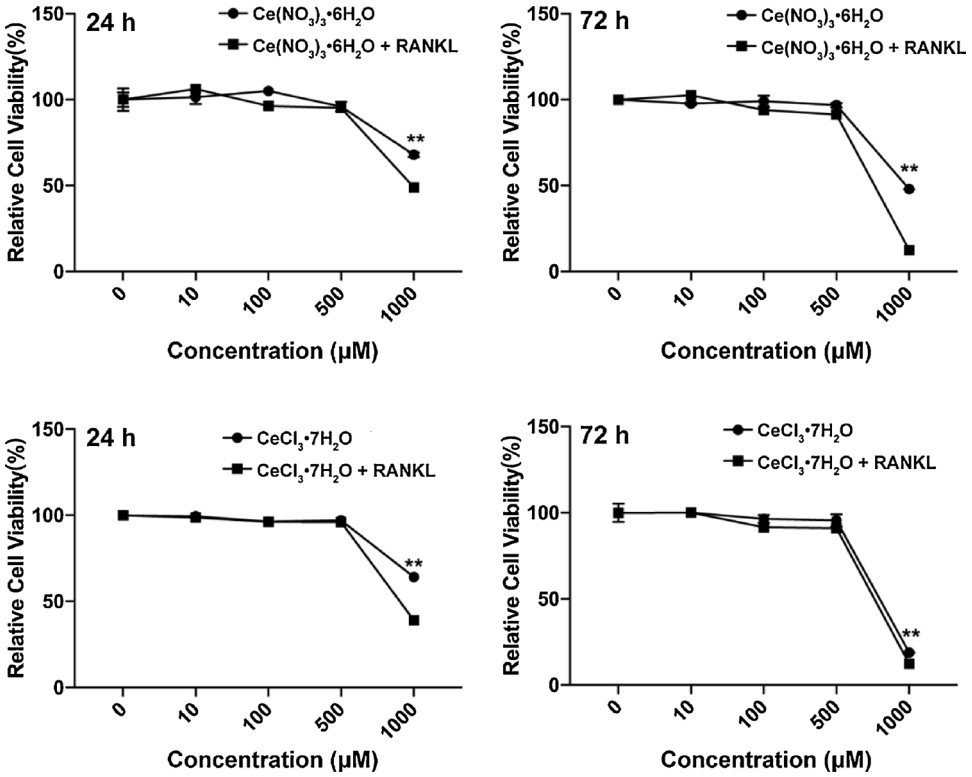


**Fig. 1.** The cell viabilities of RAW264.7 cells treated with different concentrations of cerium(III) for 24 h and 72 h with and without RANKL stimulation. Data in the figures represent the mean ± SD. ** ($p$-value < 0.01) based on one way ANOVA.

the bone metabolism homeostasis might be interfered. Recently, preliminary study has reported that cerium(III) could promote the osteogenesis through the activation of TGF-β/BMP signaling pathway of mesenchymal stem cells [19]. However, the role of cerium(III) in osteoclatogenesis still remains unknown. In this study, the effects of cerium(III) on the osteoclatogenesis were explored. The promotion of *in vitro* and *in vivo* osteoclasts differentiation by the administration of cerium(III) was illustrated. The mechanisms of cerium(III) promoted osteoclasts differentiation through the generation of ROS from Nox1 was discussed. To eliminate the possible effects of anions on the results of the experiments, Ce $(NO_3)_3{\cdot}6H_2O$ and $CeCl_3{\cdot}7H_2O$ were used as cerium(III) source.

## 2. Materials and methods

### 2.1. Chemicals and regents

The Ce $(NO_3)_3{\cdot}6H_2O$ and $CeCl_3{\cdot}7H_2O$ were purchased from Acros. Cerium(III) solution at concentrations ranging from 10 to 1000 μM were prepared immediately before using. The pre-osteoclast mouse macrophage cell line RAW264.7 was obtained from the American Type Culture Collection. Receptor activator nuclear factor-kB ligand (RANKL) and macrophage colony-stimulating factor (M-CSF) were purchased from R&D Systems. Dulbecco's modified eagle's medium (DMEM) high glucose and fetal bovine serum (FBS) were purchased from Gibico Life Technologies. Alamar blue was purchased from Invitrogen. ROS assay kit dichlorofluorescin diacetate (DCFH-DA) was purchased from Beyotime Biotechnology. Tartrate-resistant acid phosphatase (TRAP) stain kit was obtained from Sigma. Actin cytoskeleton and focal adhesion (FAK) kit was obtained from Millipore. Antibodies against NFATc-1, c-FOS, Nox1 and β-actin were purchased from Bioss.

### 2.2. Cell culture and cell viability assay

The RAW264.7 cells were grown in DMEM high glucose medium containing 8% FBS and incubated in a humidified atmosphere supplemented with 5% $CO_2$ at 37 °C. For viability assay, cells were seeded onto 96-well plates at concentration of $6 \times 10^3$ cells/well. The cells were added RANKL (50 ng/mL) and M-CSF (50 ng/mL) to induce the differentiation for 24 h, 48 h and 72 h. The concentrations of RANKL and M-CSF were kept at 50 ng/mL for all of the following experiments. The cell viability was detected by Alamar Blue kit. The fluorescence intensity with excitation wavelength at 560 nm and emission wavelength at 590 nm was detected on a Bio-Tek Synergy H4 micro-plate reader.

### 2.3. TRAP and FAK staining

The RAW264.7 cells were seeded on 96-well plates ($6 \times 10^3$ cells/well) and incubated with different concentration of cerium(III) in the presence of RANKL and M-CSF for 72 h. The medium was removed and the cells were washed twice by PBS. After that, the cells were fixed in 4% paraformaldehyde solution for 20 min and then stained by TRAP and FAK following the procedures of the manufacturer.

### 2.4. Resorption pit formation assay

Bone slices with thickness of about 100 μm were cut from bovine femoral compact bone. The slices were washed by PBS and sterilized using 75% ethanol. After drying at room temperature for 48 h, the slices were seeded RAW264.7 cells for 12 h. After that, the cells were cultured in medium containing 8% FBS, RANKL and M-CSF in the presence of different concentrations of cerium(III) for 6 days. Then the cells were removed by 0.1% sodium hypochlorite for 5 min and the bone slices were washed by PBS for 3 times. The pits were stained by toluidine blue for 1 min. The areas of the resorbed bone surface were analyzed by

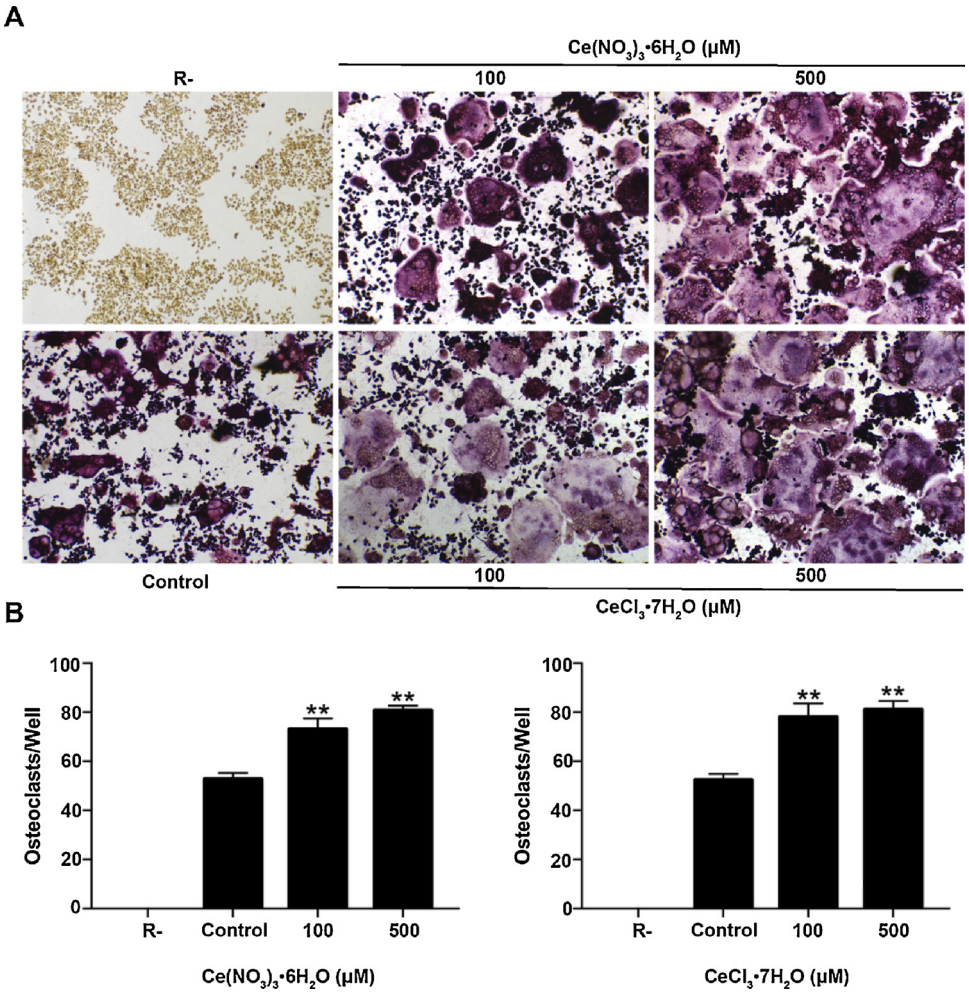


**Fig. 2.** Cerium(III) promoted the osteoclasts differentiation. (A) TRAP staining of osteoclasts treated with cerium(III) for 72 h. (B) Quantitative statistics of the stained osteoclasts based on the results of (A). Data in the figures represent the mean ± SD. ** ($p$-value < 0.01) based on one way ANOVA.

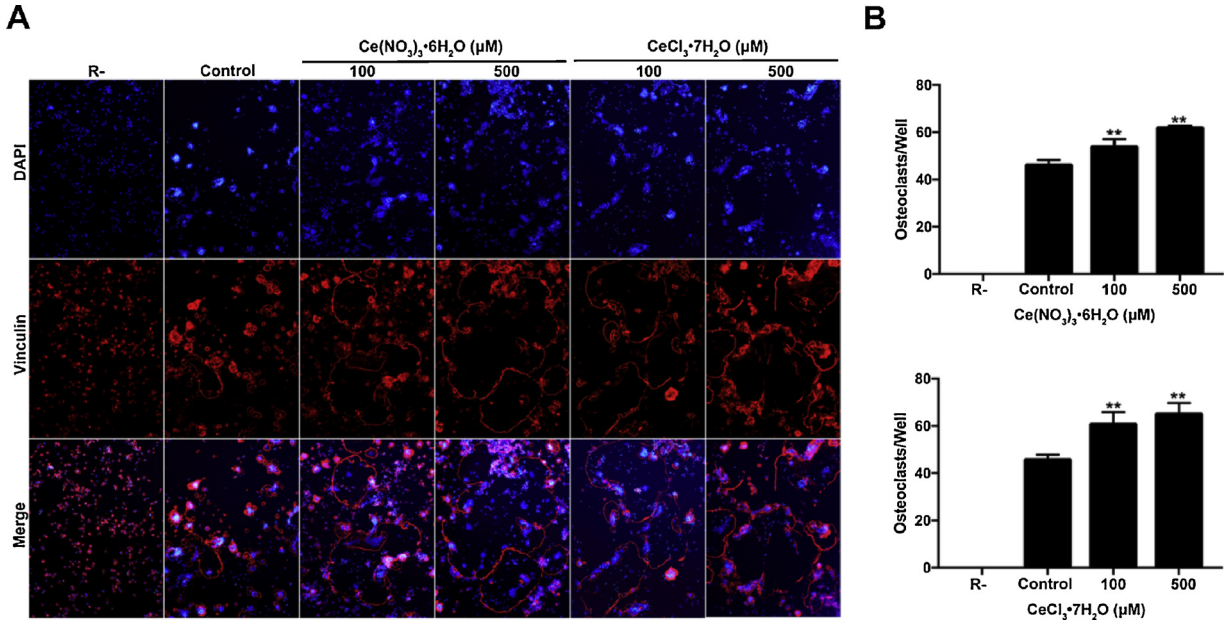


**Fig. 3.** Cerium(III) promoted the osteoclasts fusion. (A) FAK staining of osteoclasts treated with cerium(III) for 72 h. (B) Quantitative statistics of the stained osteoclasts based on the results of (A). Data in the figures represent the mean ± SD. ** ($p$-value < 0.01) based on one way ANOVA.

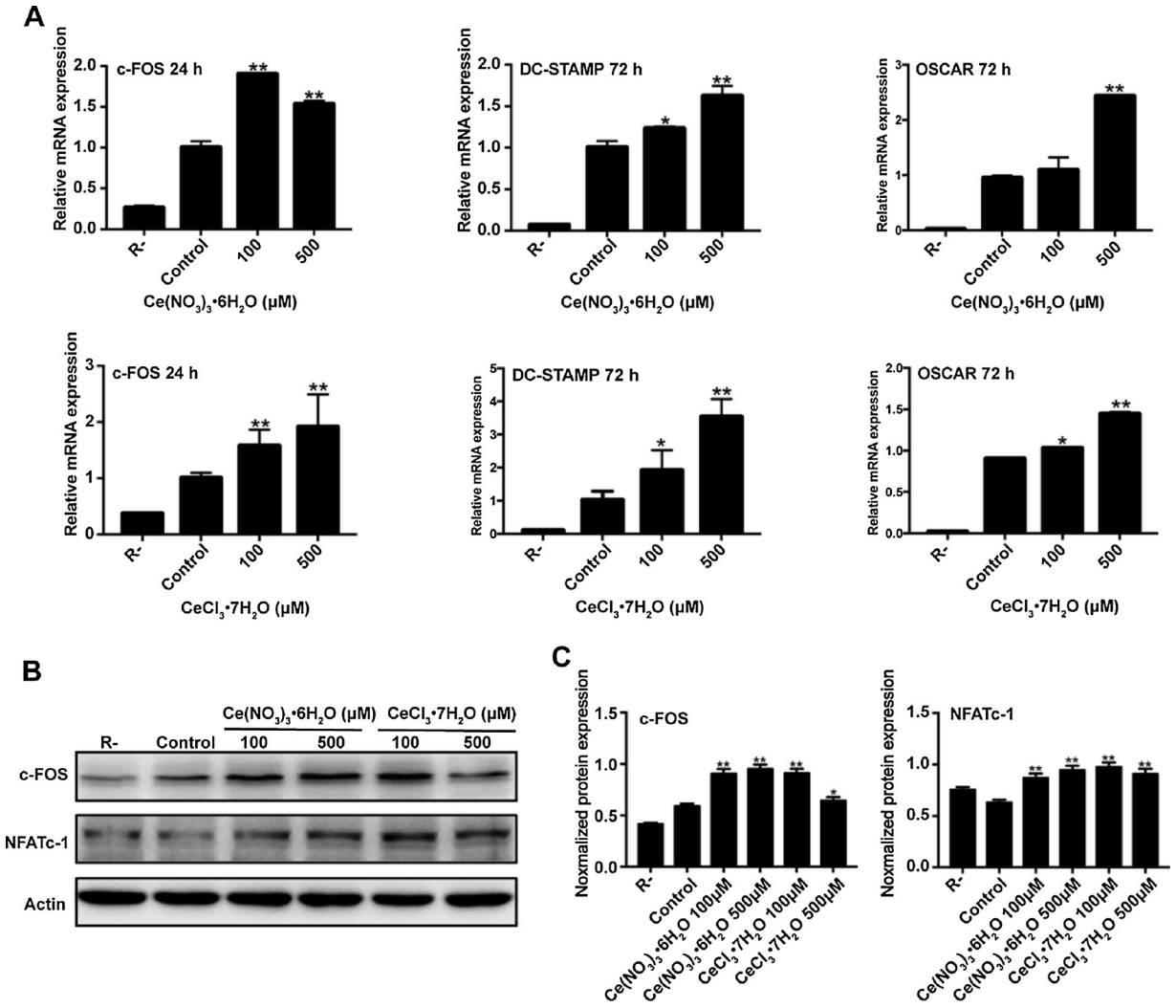


**Fig. 4.** Cerium(III) promoted the expression of osteoclasts fusion and differentiation related genes and proteins. (A) Relative mRNA expression of c-FOS, DC-STAP and OSCAR after cerium(III) treatment. (B) Western blot images of c-FOS and NFATc-1 of osteoclasts treated with cerium(III) for 24 h and 72 h respectively. (C) Relative intensity of expression level of c-FOS and NFATc-1 against β-actin. Data in the figures represent the mean ± SD. * ($p$-value < 0.05) and ** ($p$-value < 0.01) based on one way ANOVA.

Image J software.

### 2.5. Real-time quantitative PCR

The RAW264.7 cells were seeded on 24-well plates ($4 \times 10^4$ cells/well) and incubated with different concentration of cerium(III) in the presence of RANKL and M-CSF for 24 and 72 h. The total RNA was isolated by Trizol and the concentration of the RNA was detected on ultra low volume spectrometer (BioDrop, UK). The single-stranded cDNA was prepared from 1 μg of total RNA using reverse transcriptase with oligo-dT primer according to the manufacturer's instructions. The solution containing 1 μg cDNA was subjected to PCR amplification using specific primers for c-FOS, DC-STAMP, OSCAR and Nox1. All reactions were run in triplicate and were normalized to the housekeeping gene GAPDH. SYBR Green I was used as fluorescence indicator. The specific primers used for amplification were as follows: GAPDH: forward, 5′-TCTGCTGGAAGGTGGTGGACAGT-3′ and reverse, 5′−CCT CTATG CCAACACAGTGC-3′; c-Fos: forward, 5′-AACAGATCCGAGCAG CTTCTA-3′ and reverse, 5′-GACTTTCCTGTCGAATGCACT-3′; DC-STAMP: forward, 5′-TTATGTGTTTCCACGAAGCCCTA-3′ and reverse 5′-ACAGAAGAGAGAGGGCAACG-3′; OSCAR: forward, 5′-GGTCCTCAT CTGCTTG-3′ and reverse 5′-TATCTGGTGGAGTCTGG-3′; Nox1: forward, 5′-ATGCCCCTGCTGCTCGAATA-3′ and reverse 5-AAATTGCCCC TCCATTTCCT-3′.

### 2.6. Western blot assay

The RAW264.7 cells were seeded on 6-well plates ($2 \times 10^5$ cells/well) and incubated with different concentration of cerium(III) in the presence of RANKL and M-CSF for 72 h. The cells were washed by PBS for 3 times and then lysed in RIPA lysis buffer containing 50 mM Tris, 150 mM NaCl, 1% Triton X-100, 1% sodium deoxycholate, 0.1% SDS and protein inhibitor sodium orthovanadate, sodium fluoride, EDTA and leupeptin. Protein samples were subjected to SDS-PAGE and then transferred onto PVDF membranes. After blocking in 5% skim milk for 1 h at room temperature, membranes were incubated with rabbit antibodies against c-FOS, NFATc-1, Nox1 and β-actin (1:1000) at 4 °C overnight followed by 1 h incubation with secondary antibody (HRP-labeled Goat Anti-Rabbit IgG (H + L)).

### 2.7. Intracellular ROS detection

The RAW264.7 cells were seeded on 96-well plates ($6 \times 10^3$ cells/well) and incubated with different concentration of cerium(III) in the presence of RANKL and M-CSF for 72 h. After that, the cells were added 10 μM DCFH-DA at 37 °C for 20 min. The intracellular ROS was

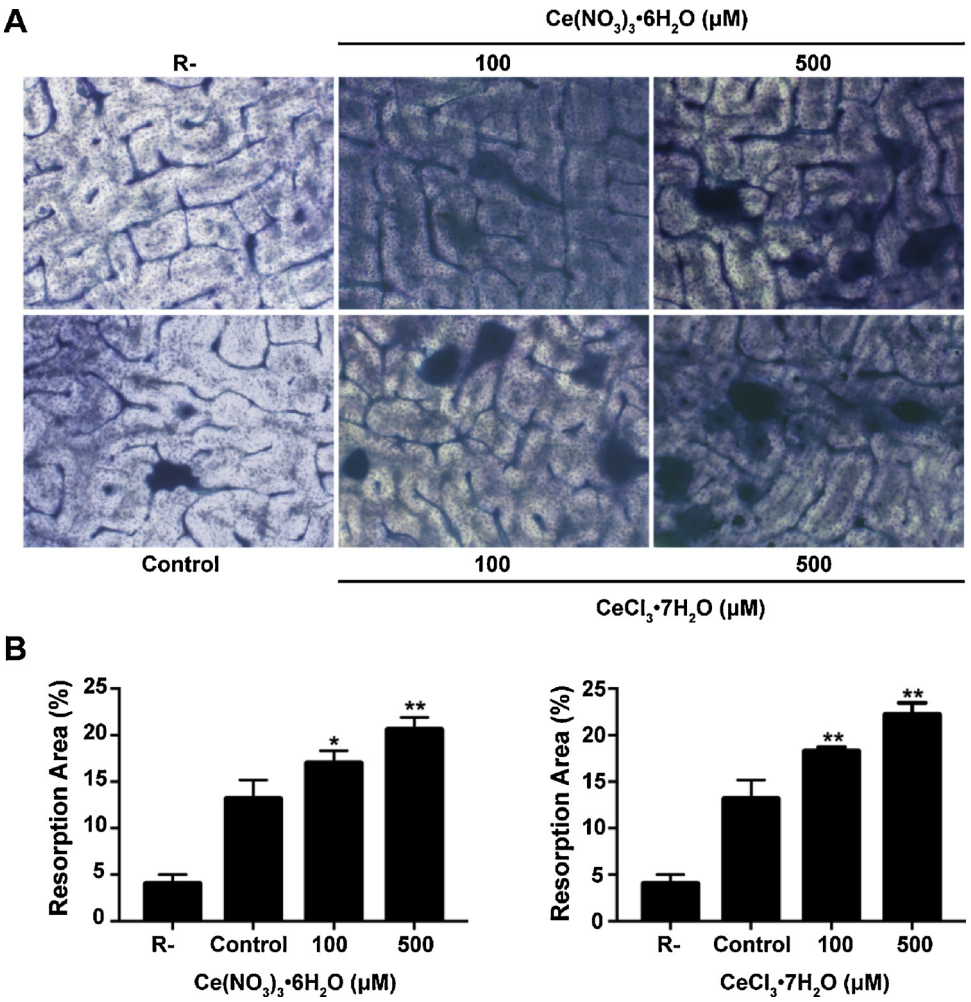


**Fig. 5.** Cerium(III) enhanced bone resorption of osteoclasts. (A) Typical images of toluidine blue stained osteoclasts resorption pits. (B) Quantitative statistics of resorption bone areas based on the results of (A). Data in the figures represent the mean ± SD. * ($p$-value < 0.05) and ** ($p$-value < 0.01) based on one way ANOVA (For interpretation of the references to colour in this figure legend, the reader is referred to the web version of this article).

observed on inverted florescence microscope and the florescence intensity was analyzed by Image J software. For quantitative intracellular ROS analysis, the cells were seeded on 12-well plates ($1 \times 10^5$ cells/well) and incubated with different concentration of cerium(III) in the presence of RANKL and M-CSF for 48 h. The florescence was detected by flow cytometer after adding DCFH-DA.

### 2.8. Mitochondrial membrane potential (MMP) detection

The RAW264.7 cells were seeded on 6-well plates ($2 \times 10^5$ cells/well) and incubated with different concentration of cerium(III) in the presence of RANKL and M-CSF for 24 h. The cells were washed once with PBS. Positive control was pretreated with 50 μM CCCP for 5 min. All the samples were stained with lipophilic dye JC-1 (2 μM) for 20 min at 37 °C containing 5% $CO_2$ [20]. Cells were rinsed once and re-suspended in 500 μL PBS for flow cytometry detecting. JC-1 was excited at 488 nm and emission singles at 535 and 595 nm were recorded to quantify the population of green and red fluorescence respectively. Frequency plots were prepared for red and green fluorescent signals to determine the percentage of normal and depolarized cells.

### 2.9. Mice and treatment

Male C57BL/6 mice (4 and 8 weeks old) were obtained from Animal Center of Army Medical University. All experimental procedures were approved by Army Medical University and performed according to guidelines of laboratory animal care and use. Each aged mice were randomly divided into 5 groups (n = 5) including control, Ce$(NO_3)_3 \cdot 6H_2O$ low dosage (10 mg/kg), Ce$(NO_3)_3 \cdot 6H_2O$ high dosage (100 mg/kg), $CeCl_3 \cdot 7H_2O$ low dosage (10 mg/kg) and $CeCl_3 \cdot 7H_2O$ high dosage (100 mg/kg). The cerium(III) were dissolved in saline and filtered with 0.22 μm membrane. The solution was injected directly onto the skull of the mouse at interval of 48 h for 9 days. All of the treated mice were sacrificed one day after the last injection.

### 2.10. Statistical analysis

Statistical significance was determined using one-way ANOVA SPSS statistics and a statistical difference was considered significant when the *p < 0.05 and **p < 0.01. Data were presented as mean ± standard deviation.

## 3. Results

### 3.1. Cytotoxicity of cerium(III)

The RAW264.7 cells were incubated with different concentrations of cerium(III) for 24 and 72 h. Alamar Blue was utilized to assess the cytotoxicity of cerium(III). As shown in Fig. 1, both Ce$(NO_3)_3 \cdot 6H_2O$ and $CeCl_3 \cdot 7H_2O$ did not inhibit the cell viability of RAW264.7 cells at

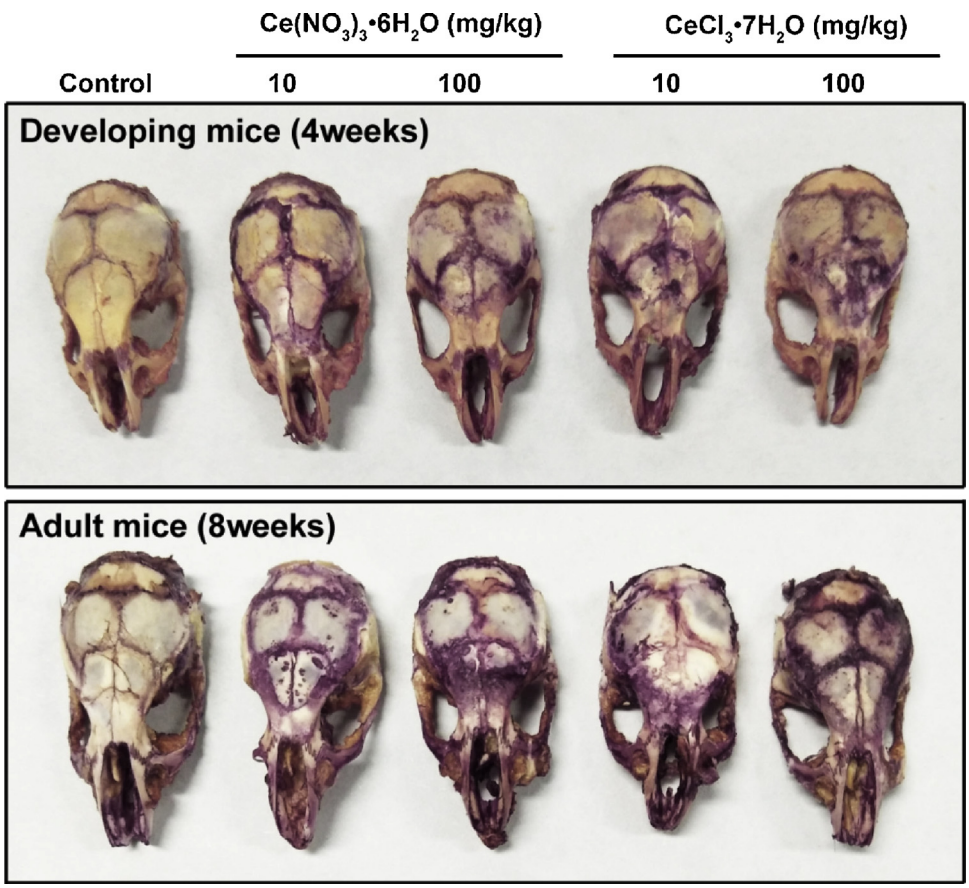


**Fig. 6.** The TRAP staining of mice skull treated with cerium(III) for 9 days.

concentration lower than 500 μM with or without RANKL and M-CSF. Based on these results, 100 and 500 μM of cerium(III) was chosen for all of the *in vitro* experiments.

### 3.2. Cerium(III) promoted osteoclastogenesis in vitro

The RAW264.7 cells seeded on 96-plates were treated with cerium (III) for 72 h in the presence of RANKL and M-CSF. The osteoclastogenesis was characterized by TRAP staining, FAK staining and osteoclasts differentiation specific gene detection. The TRAP staining results were shown in Fig. 2. The cells with more than 3 nucleuses were counted as osteoclasts. Cerium(III) significantly promoted the osteoclastogenesis as the numbers of osteoclasts formed in each 96-plates well treated with 0, 100 and 500 μM $Ce(NO_3)_3{\cdot}6H_2O$ were 49, 71 and 78 respectively, and these numbers for cells treated with 0, 100 and 500 μM $CeCl_3{\cdot}7H_2O$ were 49, 76 and 79 respectively. These results were further confirmed by FAK staining which was generally used to characterize the fusion of osteoclasts. As can be seen in Fig. 3, the numbers of osteoclasts stained by FAK in each 96-plates well treated with 0, 100 and 500 μM $Ce(NO_3)_3{\cdot}6H_2O$ were 45, 55 and 61 respectively, and these numbers for cells treated with 0, 100 and 500 μM $CeCl_3{\cdot}7H_2O$ were 45, 45 and 58 respectively. The gene detection results were shown in Fig. 4. The c-FOS was detected 24 h after cerium(III) treatment since this gene responses very quickly after the differentiation induction. The DC-STAMP and OSCAR which represent the fusion and differentiation genes were detected 72 h after cerium(III) treatment. As can be seen in the results, all of these detected genes were up-regulated after treating the cells with cerium(III). These results demonstrated that both $Ce(NO_3)_3{\cdot}6H_2O$ and $CeCl_3{\cdot}7H_2O$ could promote the osteoclastogenesis.

### 3.3. Cerium(III) enhanced bone resorption of osteoclasts

The function of the cerium(III) promoted osteoclasts was tested through pit formation assay. The RAW 264.7 cells seeded on bovine femoral compact bone in the presence of 0, 100 and 500 μM cerium(III) were cultured for 6 days to form mature osteoclasts. The resorption pits formed by the osteoclasts were stained and the resorption areas were measured for statistical analysis. As shown in Fig. 5, the pit areas for the cells treated with 0, 100 and 500 μM $Ce(NO_3)_3{\cdot}6H_2O$ were 13.1%, 16.5% and 20.1% respectively, and the pit areas for the cells treated with 0, 100 and 500 μM $CeCl_3{\cdot}7H_2O$ were13.1%, 18.2% and 22.2% respectively. These results indicated that cerium(III) not only promoted the osteoclastogenesis but also enhanced the bone resorption capability of the osteoclasts.

### 3.4. Cerium(III) activated osteoclasts in vivo

After getting the *in vitro* results that cerium(III) could promote the osteoclastogenesis, the effects of cerium(III) on the osteoclastogenesis *in vivo* was evaluated by injecting cerium(III) solution onto the skull of mice. The mice were sacrificed and their skulls were separated for TRAP staining. As can be seen in Fig. 6, adult (8 weeks) and developing mice (4 weeks) groups showed deeper TRAP colour comparing with the control group which implied that the osteoclastogenesis of mice treated by cerium(III) was significantly accelerated. Besides, the activated osteoclasts were gathered around the sutures where the bone metabolism was very active.

### 3.5. Cerium(III) rose the intracellular ROS level

It is well known that the RANKL dependent osteoclasts

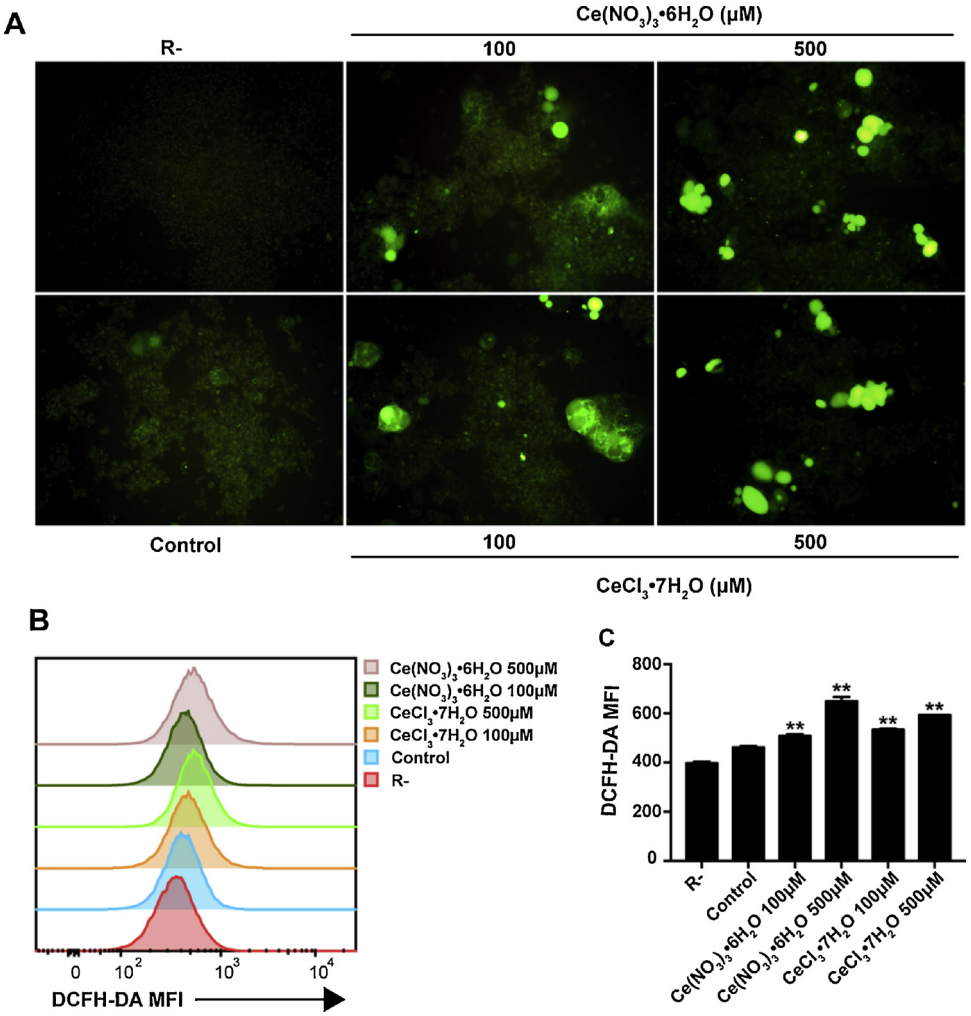


**Fig. 7.** Cerium(III) increased the intracellular ROS level of osteoclasts. (A) ROS probe DCFH-DA stained osteoclasts treated with cerium(III) for 72 h. (B) MFI of osteoclasts treated with cerium(III) for 48 h. (C) MFI quantitative statistics of osteoclasts treated with cerium(III) for 48 h. Data in the figures represent the mean ± SD. ** ($p$-value < 0.01) based on one way ANOVA.

differentiation is accompanied with the change of intracellular ROS level [21,22]. Thus, the cerium(III) induced enhancement of osteoclasts differentiation could be caused by the change of ROS level. To prove this hypothesis, the ROS change in osteoclasts was detected by flow cytometry and fluorescence microscope using DCFH-DA probe. As shown in Fig. 7, the negative control without the addition of RANKL showed weak fluorescence intensity due to the low intracellular ROS level. Once the differentiation was initiated by the addition of RANKL, increase of intracellular ROS level was observed. Most importantly, the addition of cerium(III) further increased the ROS level of the cells. These results were confirmed by quantitative fluorescence detection where flow cytometer was used to measure the mean fluorescence intensity (MFI) of the cells. As shown in Fig. 7, the MFI of cells treated with cerium(III) was much higher than that of the control. These results demonstrated that cerium(III) could significantly rise the intracellular ROS level in the process of osteoclasts differentiation.

### 3.6. Cerium(III) enhanced the expression of Nox1

ROS can be generated and modulated by many pathways in cells. Within these pathways, the Nox1 derived ROS is essential for the differentiation of osteoclasts [23–25]. Thus, the enhanced expression of Nox1 might be the reason for the rise of ROS level in osteoclasts. To investigate the effects of cerium(III) on the expression of Nox1, the cells were cultured with cerium(III) in the presence of RANKL and M-CSF for 72 h. The mRNA and protein expression levels of Nox1 were detected by qPCR and WB. As shown in Fig. 8, both of the mRNA and protein levels of Nox1 were significantly increased after treating the cells with cerium (III).

### 3.7. Cerium(III) caused the depolarization of mitochondria

Except for the expression of Nox1, the activity of this protein is another critical parameter that could modulate its ROS generation capability. To detect the activity of Nox1 by measuring the change of MMP, the RAW264.7 cells were incubated with different concentrations of cerium(III) for 24 h, and the MMP of the cells were analyzed by JC-1 mitochondria staining kit. As shown in Fig. 9, loss of MMP in the cells cultured in the presence of cerium(III) was observed. The percentages of the depolarized cells cultured with 100 and 500 μM $Ce(NO_3)_3{\cdot}6H_2O$ were 58.3% and 56.4%, and the values for cells cultured with 100 and 500 μM $CeCl_3{\cdot}7H_2O$ were 59.1% and 62.0%. As control, the percentage of depolarized cells in normal culture condition was 47.4%. These results indicated that cerium(III) could significantly increase the MMP depolarization of the osteoclasts.

## 4. Discussion

The extensive use of cerium(III) salt has increased the opportunity that people expose to cerium(III).It has been reported that the cerium

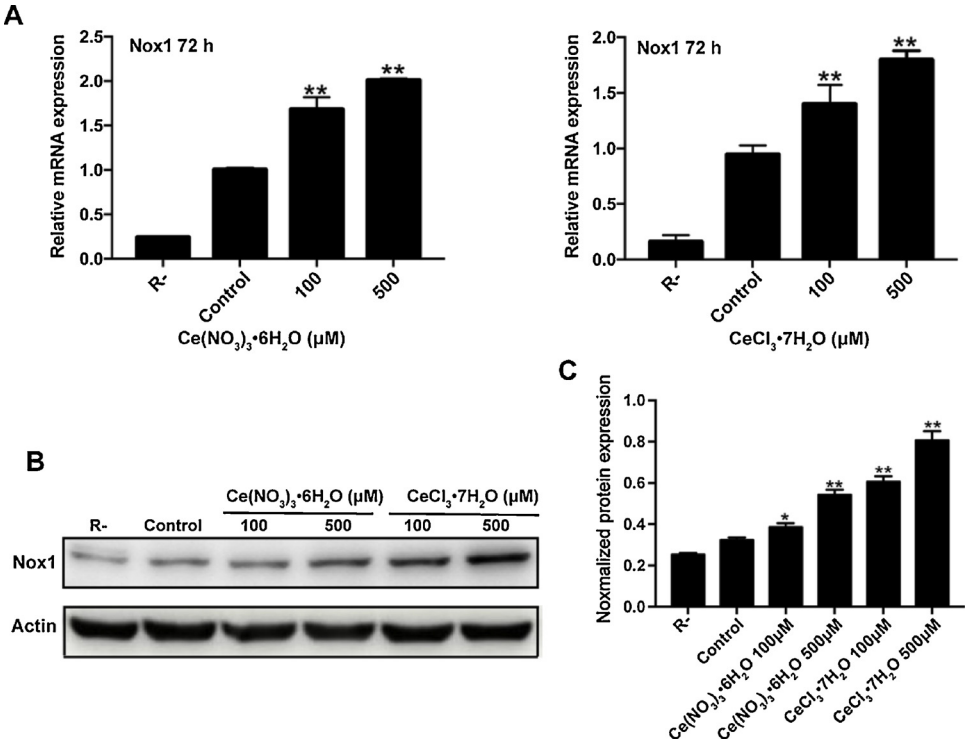


**Fig. 8.** Cerium(III) promoted the expression of Nox1. (A) Relative mRNA expression of Nox1 of osteoclasts treated with cerium(III) for 72 h. (B) Western blot images of Nox1 and β-actin of osteoclasts treated with cerium(III) for 72 h. (C) Relative intensity of expression level of Nox1 against β-actin. Data in the figures represent the mean ± SD. * ($p$-value < 0.05) and ** ($p$-value < 0.01) based on one way ANOVA.

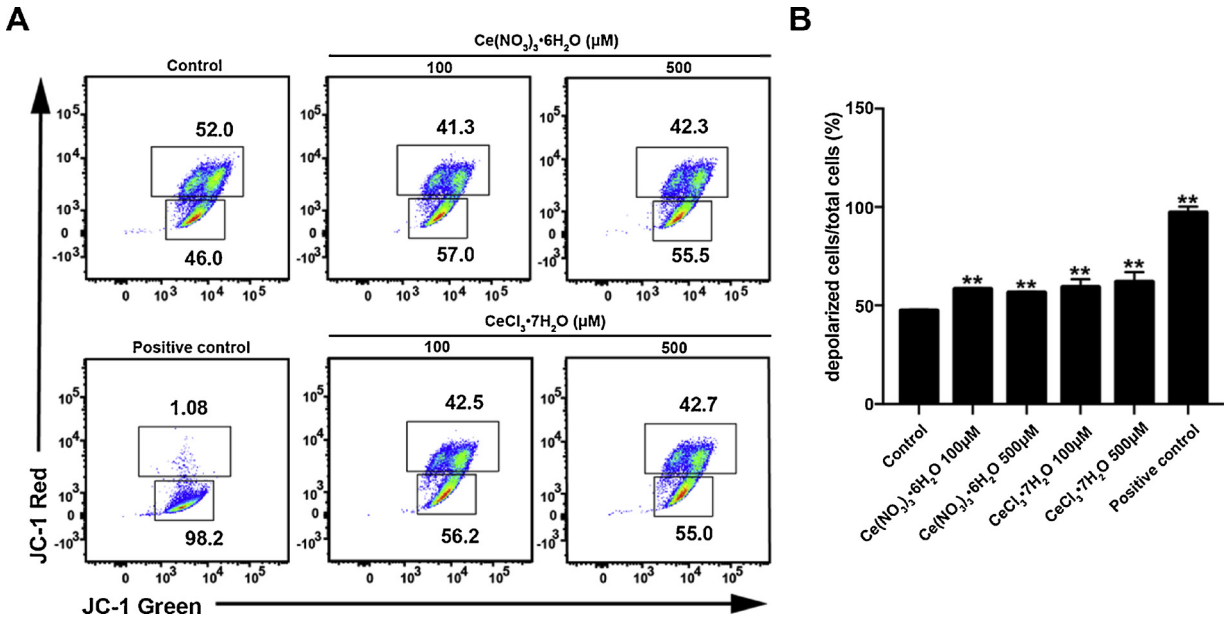


**Fig. 9.** Cerium(III) decreased the MMP of osteoclasts. (A) Percentage of osteoclasts in conditions of resting potential and action potential after 24 h treatment of cerium(III). (B) Quantitative statistics of the percentage of the depolarized cells based on the result of (A). Data in the figures represent the mean ± SD. ** ($p$-value < 0.01) based on one way ANOVA.

(III) ions were mainly deposited in bone skeletal system due to their similar ionic radius to calcium(II) ions [6]. Thus, the reveal of the potential effects of cerium(III) ion on the skeletal system metabolism homeostasis is of great importance. However, little attention has been paid to these works. In the present study, we studied the effects of cerium(III) on the osteoclastogenesis. To eliminate any confusion that might be caused by the anions, two kinds of cerium(III) salts Ce $(NO_3)_3{\cdot}6H_2O$ and $CeCl_3{\cdot}7H_2O$ were used in the study.

The effects of cerium(III) on the osteoclastogenesis were characterized by several experiments including TRAP staining, FAK staining, osteoclasts differentiation related mRNA and protein detection. The promotion of osteoclastogenesis induced by cerium(III) was observed in all of these experiments. The TRAP (Fig. 2) and FAK (Fig. 3) staining showed more osteoclasts formation with the addition of cerium(III). The osteoclasts differentiation related mRNA expression such as c-FOS, DC-STAMP and OSCAR were increased (Fig. 4), and the protein expressions of c-FOS and NFATc-1 which represent the typical osteoclasts differentiation processes were also increased with the addition of cerium(III) (Fig. 4) [26]. The function of the cerium(III) treated osteoclasts was evaluated by the resorption of bovine femoral compact bone for 6 days [27.28]. The resorption pit areas formed by the osteoclasts with cerium(III) treatment were obviously higher than

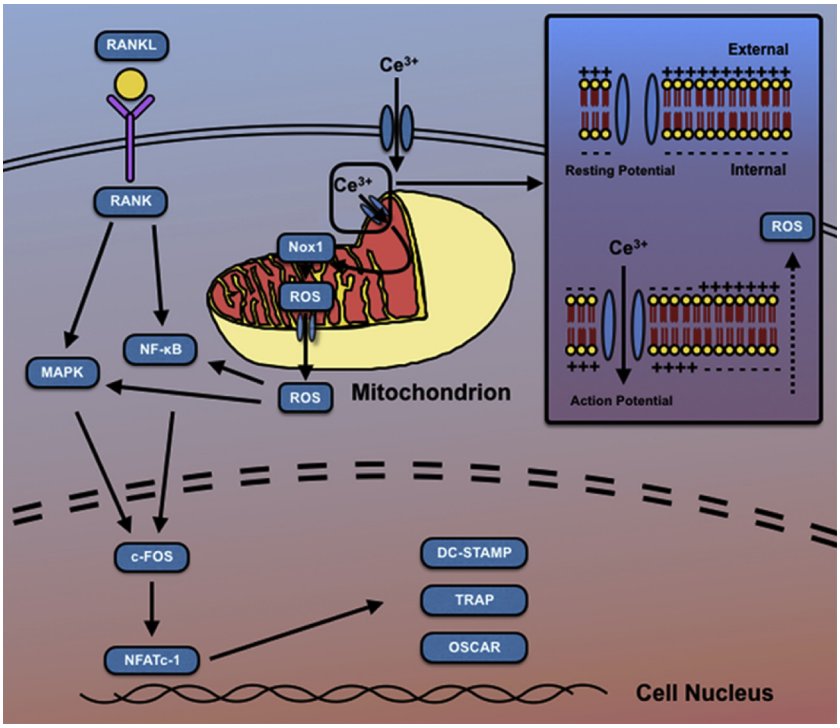


**Fig. 10.** Scheme illustrated the mechanism of cerium(III) promoted osteoclastogenesis.

the control (Fig. 5). Most importantly, the skull of mice treated with cerium(III) exhibited enhanced activation of osteoclasts gathering around the sutures (Fig. 6). Taking together, these results provided strong evidences that cerium(III) could promote the osteoclastogenesis.

It has been reported that the RANKL dependent osteoclasts differentiation is accompanied with the rise of intracellular ROS level [22], and the addition of ROS scavengers could inhibit the osteoclasts differentiation [21,27–29]. It is therefore reasonable to believe that the cerium(III) induced promotion of osteoclasts differentiation might be ascribed to the rise of intracellular ROS level. To prove this hypothesis, the osteoclasts treated with and without cerium(III) were sent for ROS detection. As expected, significant ROS level augmentation was observed in cerium(III) treated cells (Fig. 7). We next traced back to explore the source of ROS generation induced by cerium(III). ROS can be generated by multiple proteins within cell such as xanthine oxidase, lipoxygenase, cytochrome P-450 and nitric oxide synthase [30–33]. Within these proteins, Nox family are extraordinary as these proteins produce ROS on only one side of the lipid bilayer, and the ROS generated from Nox are confined to the localizations where the Nox-dependent ROS signaling pathways take place [34]. Besides, unlike the other proteins that generate ROS as byproducts, Nox generate ROS as major products. Further, recent studies have found that the Nox1 derived ROS are essential for osteoclasts differentiation [23–25]. We thus detected the change of Nox1 expression of osteoclasts treated with cerium(III). As expected, the mRNA and protein expression of Nox1 were enhanced after treating the cells with cerium(III) (Fig. 8). Except for the expression level, we also detected the activity of Nox1 through measuring the depolarization of mitochondria based on the principle that a slight depolarization leads to the initiation of Nox and the activity of Nox increases with the enhancement of mitochondrial MMP depolarization [35,36]. As a result, the osteoclasts treated with cerium (III) showed a significant increase in mitochondria MMP depolarization (Fig. 9). These results implied that the rise of ROS level could be ascribed to the cerium(III) stimulated enhancement of expression and activity of Nox1. The rise of ROS level could later promote the osteoclasts differentiation through the enhancement of RANKL signaling pathways.

In conclusion, cerium(III) ions could promote the RANKL dependent osteoclastogenesis characterized by TRAP and FAK staining as well as osteoclasts differentiation related genes and proteins expression. Anions associated with the cerium(III) have no effects on the differentiation of osteoclasts. The cerium(III) promoted osteoclasts exhibited enhanced bone resorption capability. The mechanism underlying the promotion of osteoclastogenesis was ascribed to the cerium(III) stimulated enhancement of expression and activity of Nox1 which caused the elevation of ROS level in the osteoclasts (Fig. 10). This study provided fundamental information for recognizing the potential effects of cerium (III) on the metabolism homeostasis of skeletal system which could be useful for future application of cerium(III) in biomedical researches.

## Conflicts of interest statement

None declared.

## Acknowledgements

This work was supported by the National Natural Science Foundation of China (81471782 and 31470870).

## References

[1] T. Montini, M. Melchionna, M. Monai, P. Fornasiero, Fundamentals and catalytic applications of CeO2-based materials, Chem. Rev. 116 (2016) 5987–6041.
[2] A. Ali, A. Rafique, M. Kaleemullah, G. Abbas, M. Ajmal Khan, M.A. Ahmad, R. Raza, Effect of alkali carbonates (single, binary, and ternary) on doped ceria: a composite electrolyte for low-temperature solid oxide fuel cells, ACS Appl. Mater. Interfaces 10 (2018) 806–818.
[3] P.T.M. Pham, T.L. Minh, T.T. Nguyen, I. Van Driessche, Ceo(2) based catalysts for the treatment of propylene in motorcycle's exhaust gases, Materials (Basel) 7 (2014) 7379–7397.
[4] J.A. Rodriguez, D.C. Grinter, Z. Liu, R.M. Palomino, S.D. Senanayake, Ceria-based model catalysts: fundamental studies on the importance of the metal-ceria interface in CO oxidation, the water-gas shift, CO2 hydrogenation, and methane and alcohol reforming, Chem. Soc. Rev. 46 (2017) 1824–1841.
[5] A. Younis, D. Chu, Y.V. Kaneti, S. Li, Tuning the surface oxygen concentration of surrounded ceria nanocrystals for enhanced photocatalytic activities, Nanoscale 8 (2016) 378–387.
[6] M.A. Jakupec, P. Unfried, B.K. Keppler, Pharmacological properties of cerium

compounds, Rev. Physiol. Biochem. Pharmacol. 153 (2005) 101–111.
[7] N. Kayashima, T. Hayama, [Effectiveness of several antiemetics in vomiting induced by orally administrated copper sulfate in cats and dogs], Nihon Yakurigaku Zasshi 72 (1976) 293–296.
[8] S.M. Scholten-Jaegers, M.K. Nieuwenhuis, M.E. van Baar, A.S. Niemeijer, J. Hiddingh, G.I. Beerthuizen, Epidemiology and outcome of patients with Burns treated with cerium nitrate silversulfadiazine, J. Burn Care Res. 38 (2017) e432–e442.
[9] D. Oro, T. Yudina, G. Fernandez-Varo, E. Casals, V. Reichenbach, G. Casals, B. Gonzalez de la Presa, S. Sandalinas, S. Carvajal, V. Puntes, W. Jimenez, Cerium oxide nanoparticles reduce steatosis, portal hypertension and display anti-inflammatory properties in rats with liver fibrosis, J. Hepatol. 64 (2016) 691–698.
[10] J. Hong, X. Yu, X. Pan, X. Zhao, L. Sheng, X. Sang, A. Lin, C. Zhang, Y. Zhao, S. Gui, Q. Sun, L. Wang, F. Hong, Pulmonary toxicity in mice following exposure to cerium chloride, Biol. Trace Elem. Res. 159 (2014) 269–277.
[11] H. Zhao, J. Cheng, J. Cai, Z. Cheng, Y. Cui, G. Gao, R. Hu, X. Gong, L. Wang, F. Hong, Liver injury and its molecular mechanisms in mice caused by exposure to cerium chloride, Arch. Environ. Contam. Toxicol. 62 (2012) 154–164.
[12] X. Wang, J. Su, L. Zhu, N. Guan, X. Sang, Y. Ze, X. Zhao, L. Sheng, S. Gui, Q. Sun, L. Wang, F. Hong, Hippocampal damage and alterations of inflammatory cytokine expression in mice caused by exposure to cerium chloride, Arch. Environ. Contam. Toxicol. 64 (2013) 545–553.
[13] X. Sang, X. Ze, S. Gui, X. Wang, J. Hong, Y. Ze, X. Zhao, L. Sheng, Q. Sun, X. Yu, L. Wang, F. Hong, Kidney injury and alterations of inflammatory cytokine expressions in mice following long-term exposure to cerium chloride, Environ. Toxicol. 29 (2014) 1420–1427.
[14] J.E. Allison, C. Boutin, D. Carpenter, D.M. Ellis, J.L. Parsons, Cerium chloride heptahydrate (CeCl3. 7H2O) induces muscle paralysis in the generalist herbivore, Melanoplus sanguinipes (Fabricius) (Orthoptera: acrididae), fed contaminated plant tissues, Chemosphere 120 (2015) 674–679.
[15] K. Matsuo, N. Irie, Osteoclast-osteoblast communication, Arch. Biochem. Biophys. 473 (2008) 201–209.
[16] S.L. Teitelbaum, Bone resorption by osteoclasts, Science 289 (2000) 1504–1508.
[17] M. Ishii, J.G. Egen, F. Klauschen, M. Meier-Schellersheim, Y. Saeki, J. Vacher, R.L. Proia, R.N. Germain, Sphingosine-1-phosphate mobilizes osteoclast precursors and regulates bone homeostasis, Nature 458 (2009) 524–528.
[18] T.T. To, P.E. Witten, A. Huysseune, C. Winkler, An adult osteopetrosis model in medaka reveals the importance of osteoclast function for bone remodeling in teleost fish, Comp. Biochem. Physiol. C Toxicol. Pharmacol. 178 (2015) 68–75.
[19] D.D. Liu, J.C. Zhang, Q. Zhang, S.X. Wang, M.S. Yang, TGF-beta/BMP signaling pathway is involved in cerium-promoted osteogenic differentiation of mesenchymal stem cells, J. Cell. Biochem. 114 (2013) 1105–1114.
[20] M.I. Khan, A. Mohammad, G. Patil, S.A. Naqvi, L.K. Chauhan, I. Ahmad, Induction of ROS, mitochondrial damage and autophagy in lung epithelial cancer cells by iron oxide nanoparticles, Biomaterials 33 (2012) 1477–1488.
[21] S. Srinivasan, A. Koenigstein, J. Joseph, L. Sun, B. Kalyanaraman, M. Zaidi, N.G. Avadhani, Role of mitochondrial reactive oxygen species in osteoclast differentiation, Ann. N. Y. Acad. Sci. 1192 (2010) 245–252.
[22] D.A. Callaway, J.X. Jiang, Reactive oxygen species and oxidative stress in osteoclastogenesis, skeletal aging and bone diseases, J. Bone Miner. Metab. 33 (2015) 359–370.
[23] N.K. Lee, Y.G. Choi, J.Y. Baik, S.Y. Han, D.W. Jeong, Y.S. Bae, N. Kim, S.Y. Lee, 'A crucial role for reactive oxygen species in RANKL-induced osteoclast differentiation, Blood 106 (2005) 852–859.
[24] H. Sasaki, H. Yamamoto, K. Tominaga, K. Masuda, T. Kawai, S. Teshima-Kondo, K. Rokutan, NADPH oxidase-derived reactive oxygen species are essential for differentiation of a mouse macrophage cell line (RAW264.7) into osteoclasts, J. Med. Invest. 56 (2009) 33–41.
[25] I.S. Kang, C. Kim, NADPH oxidase gp91(phox) contributes to RANKL-induced osteoclast differentiation by upregulating NFATc1, Sci. Rep. 6 (2016) 38014.
[26] K. Okamoto, T. Nakashima, M. Shinohara, T. Negishi-Koga, N. Komatsu, A. Terashima, S. Sawa, T. Nitta, H. Takayanagi, Osteoimmunology: the conceptual framework unifying the immune and skeletal systems, Physiol. Rev. 97 (2017) 1295–1349.
[27] C. Dou, Z. Cao, N. Ding, T. Hou, F. Luo, F. Kang, X. Yang, H. Jiang, Z. Xie, M. Hu, J. Xu, S. Dong, Cordycepin prevents bone loss through inhibiting osteoclastogenesis by scavenging ROS generation, Nutrients 8 (2016) 231.
[28] C. Dou, J. Li, F. Kang, Z. Cao, X. Yang, H. Jiang, B. Yang, J. Xiang, J. Xu, S. Dong, Dual effect of Cyanidin on RANKL-induced differentiation and fusion of osteoclasts, J. Cell. Physiol. 231 (2016) 558–567.
[29] Y. Chen, J. Sun, C. Dou, N. Li, F. Kang, Y. Wang, Z. Cao, X. Yang, S. Dong, Alliin attenuated RANKL-induced osteoclastogenesis by scavenging reactive oxygen species through inhibiting Nox1, Int. J. Mol. Sci. (2016) 17.
[30] M.H. Ben-Mahdi, P.M. Dang, M.A. Gougerot-Pocidalo, Y. O'Dowd, J. El-Benna, C. Pasquier, Xanthine oxidase-derived ROS display a biphasic effect on endothelial cells adhesion and FAK phosphorylation, Oxid. Med. Cell. Longev. 2016 (2016) 9346242.
[31] D.Y. Chuang, A. Simonyi, P.T. Kotzbauer, Z. Gu, G.Y. Sun, Cytosolic phospholipase A2 plays a crucial role in ROS/NO signaling during microglial activation through the lipoxygenase pathway, J. Neuroinflammation 12 (2015) 199.
[32] R.V. Priyadarsini, S. Nagini, Quercetin suppresses cytochrome P450 mediated ROS generation and NFkappaB activation to inhibit the development of 7,12-dimethylbenz[a]anthracene (DMBA) induced hamster buccal pouch carcinomas, Free Radic. Res. 46 (2012) 41–49.
[33] S.R. Potje, Z. Chen, S.D.S. Oliveira, L.M. Bendhack, R.S. da Silva, M.G. Bonini, C. Antoniali, R.D. Minshall, Nitric oxide donor [Ru(terpy)(bdq)NO](3+) induces uncoupling and phosphorylation of endothelial nitric oxide synthase promoting oxidant production, Free Radic. Biol. Med. 112 (2017) 587–596.
[34] N.Y. Spencer, J.F. Engelhardt, The basic biology of redoxosomes in cytokine-mediated signal transduction and implications for disease-specific therapies, Biochemistry 53 (2014) 1551–1564.
[35] L.M. Henderson, J.B. Chappell, O.T. Jones, Superoxide generation by the electrogenic NADPH oxidase of human neutrophils is limited by the movement of a compensating charge, Biochem. J. 255 (1988) 285–290.
[36] T.E. DeCoursey, D. Morgan, V.V. Cherny, The voltage dependence of NADPH oxidase reveals why phagocytes need proton channels, Nature 422 (2003) 531–534.